Biomedicine & Pharmacotherapy 150 (2022) 112978

Contents lists available at ScienceDirect

Biomedicine & Pharmacotherapy

journal homepage: www.elsevier.com/locate/biopha

Astragaloside IV alleviates PM2.5-caused lung toxicity by inhibiting inflammasome-mediated pyroptosis via NLRP3/caspase-1 axis inhibition in mice

Demei Huang [a,1], Shihua Shi [a,1], Yilan Wang [a], Xiaomin Wang [a], Zherui Shen [a], Mingjie Wang [a], Caixia Pei [a], Yongcan Wu [a], Yacong He [b,*], Zhenxing Wang [a,**]

[a] Hospital of Chengdu University of Traditional Chinese Medicine, Chengdu 610075, China
[b] School of Pharmacy, Chengdu University of Traditional Chinese Medicine, Chengdu 611137, China

ARTICLE INFO

Keywords:
Lung toxicity
PM2.5
Astragaloside IV
Pyroptosis
NLRP3/caspase-1 axis
NLRP3 inflammasome

ABSTRACT

Exposure to particulate matter (PM)2.5 in air pollution is a serious health issue worldwide. At present, effective prevention measures and modalities of treatment for PM2.5-caused lung toxicity are lacking. This study elucidated the protective effect of astragaloside IV (Ast), a natural product from *Astragalus membranaceous* Bunge, against PM2.5-caused lung toxicity and its possible molecular mechanisms. The mice model of lung toxicity was performed by intratracheal instillation of PM2.5 dust suspension. The investigation was performed with Ast or in combination with nigericin, which is a NOD-like receptor protein 3 (NLRP3) activator. The results revealed that PM2.5 lead significant lung inflammation and promoted the pyroptosis pattern of cell death by upregulating pro-inflammatory cytokines and causing oxidative stress related to the NLRP3 inflammasome-mediated pyroptosis pathway. Ast protected against PM2.5 resulted lung toxicity via suppressing NLRP3 inflammasome-mediated pyroptosis via NLRP3/caspase-1 axis inhibition, thereby protecting the lung against PM2.5-induced lung inflammation and oxidative damage, eventually resulting in prolonged survival in mice. Nigericin partially reversed the protective effects of Ast. The present research provides new insights into the therapeutic potential of Ast, demonstrating that it might be a possible candidate for the prevention of PM2.5-caused respiratory diseases. Targeting the NLRP3 inflammasome might be a novel therapeutic tactic for PM2.5-caused respiratory diseases.

1. Introduction

Particulate matter (PM) is a mix ingredient of pollutants suspended in the air, and numerous researchers have shown that exposure to air pollution is a major contributor to the global burden of disease [1,2]. PM2.5, the diameter less or equal than 2.5 μm, may be the most harmful environmental risk factor to human health [3,4]. PM2.5 can adsorb a large number of chemical constituents, including polycyclic aromatic hydrocarbons, heavy metals, and elemental carbon, which have a variety of negative effects on human health, such as respiratory diseases, cardiovascular diseases, cancer, and non-communicable diseases [5,6]. The main health effect of exposure to fine PM is on the respiratory system, so inhalation of PM2.5 is of great concern [7]. The major toxic mechanism of PM2.5 in the pulmonary system is the inflammatory response, which can lead to a variety of acute and chronic respiratory system diseases [8]. Nevertheless, the clarification of mechanism of PM2.5-induced lung toxicity is yet to be made.

Pyroptosis is a newly recognized type of inflammatory programmed cell death, and characterized by swollen cells, forming holes on plasma membranes, and pro-inflammatory cytokine release [9,10]. The NOD-like receptor protein 3 (NLRP3) inflammasome is to be pivotal in pyroptosis. The NLRP3 inflammasome consists of NLRP3, the adapter protein ASC, and inflammatory caspase-1 [11]. Activation of inflammasomes, such as the NLRP3 inflammasome, promotes the pro-caspase-1 to converts to active cleaved form caspase-1 and subsequently controls the pro-interleukin (IL)− 1β and pro-IL-18 precursors to cleaves into their mature forms and causes pyroptosis [12]. Cell membrane recognition receptors can recognize inflammatory signals, such as

* Correspondence to: School of Pharmacy, Chengdu University of Traditional Chinese Medicine, No. 1166 Liutai Avenue, Chengdu 611137, China.
** Correspondence to: Hospital of Chengdu University of Traditional Chinese Medicine, No. 39, Shi-er-qiao Road, Chengdu 610072, China.
E-mail addresses: heyacong@126.com (Y. He), wangzhenxing@cdutcm.edu.cn (Z. Wang).
[1] These authors contributed equally to this work.

https://doi.org/10.1016/j.biopha.2022.112978
Received 23 December 2021; Received in revised form 7 April 2022; Accepted 13 April 2022
Available online 22 April 2022

the NLRP3 inflammasome, and bind to caspase-1 through the adapter protein ASC, forming a multiprotein complex and initiating to assembly to activate caspase-1 [13]. The activated caspase-1 cleaves GasderminD (GSDMD) and forms a peptide that contains the N-terminal GSDMD domain, triggering perforation and rupture of cell membrane [14]. Then, inflammatory factors are released, causing the inflammatory response. Recently, a few studies have indicated that NLRP3-associated pyroptosis may regulate lung inflammation, and release of various inflammatory factors has been implicated in acute lung injury [15,16], airway inflammation [17,18], pulmonary fibrosis [19,20], lung cancer [21,22], and other respiratory disorders. Moreover, PM2.5 activates the NLRP3 inflammasome and nuclear factor (NF)-κB signaling to regulate the secretion of pro-inflammatory cytokines in vivo [23–26]. In addition, NLRP3 inflammasome inhibitors can inhibit the pulmonary inflammatory immune response induced by PM2.5 [23]. Given its paramount importance in disease pathogenesis, the NLRP3-associated pyroptosis pathway may be a possible therapeutic target in a variety of inflammatory disorders induced by PM2.5 exposure.

As a commonly medicine-food homology specie, *Astragalus membranaceous* Bunge has been used both in daily cuisine and in clinical practice to prevent exogenous pathogenic factors in China [27,28]. Astragaloside IV (Ast), as the main component of *Astragalus membranaceous* Bunge, has pleiotropic effects, such as antioxidant, anti-inflammation, and anti-apoptotic effects [29]. Previous research has indicated that Ast provides protection by downregulating the NLRP3 inflammasome pathway in animal models [30]. However, Ast has rarely been reported to prevent PM2.5-induced pulmonary diseases by regulating NLRP3/caspase-1 signaling pathway-mediated pyroptosis. Although pyroptosis might be a vital mechanism of PM2.5 attacked lung toxicity, no in-vivo evidence is available to support this [26,31]. Thus, the purpose of this research is to explore the potential role of pyroptosis in PM2.5 caused lung toxicity, as well as the pharmacological mechanisms of Ast pre-administration in mice.

2. Materials and methods

2.1. Reagents

Ast (purity more than 98.8%) was provided by Munster Technology (Chengdu, China). PM2.5 standards (SRM 2786) were respectively offered by the National Institute of Standards and Technology (MD, USA). Nigericin sodium salt was provided by Selleck Chemicals (Houston, Texas, USA). Primary antibodies against NLRP3 (ab263899), ASC2/ASC1 (ab47092), pro-caspase-1 (ab179515), GSDMD (ab219800), NF-κB p65 (ab32536), p-p65 (ab86299), IκBα (ab32518), and GAPDH (ab181602), as well as a secondary antibody against horseradish peroxidase (ab205718), were provided by Abcam (Cambridge, UK). Antibodies against cleaved caspase-1 (AF-4022) and cleaved IL-1β (AF-4006) were purchased from Affinity Biosciences (Beijing, China). Other antibodies against cleaved GSDMD (#10137) and p-IκBα (#2859 S) were provided by Cell Signaling Technology (CST, CT, USA). Lactate dehydrogenase (LDH) myeloperoxidase (MPO), Malondialdehyde (MDA), as well as superoxide dismutase (SOD) kits were bought from Nanjing Jiancheng Biological Co. Ltd. (Nanjing, China). Multisciences (Hangzhou, China) provided the IL-18, IL-1β, IL-6, and tumor necrosis factor-alpha (TNF-α) enzyme-linked immunosorbent assay (ELISA) kits. The terminal deoxynucleotidyl transferase dUTP nick-end labeling (TUNEL) kit was obtained from Hoffmann-La Roche (Basel, Switzerland).

2.2. Animals

Healthy male C57BL/6 mice, 6–8-week-old, weighing 20–22 g, were supplied by Chendu Dossy Experimental Animals Co. Ltd. (Chengdu, China) and used as research objects in this study. All mice, with free access to water and standard diet, were kept in laboratory with 12 h dark/light cycle, a relative humidity of 55% ± 5%, a temperature of 25 °C ± 1 ℃ for 1 week to adapt to the environment before the experiment. The animal research was conducted in line with the regulations of the Animal Ethics Committee of Chengdu University of Traditional Chinese Medicine. The animal welfare was in line with the relevant international standards for experimental animals.

2.3. Experimental design

Mice were randomly assigned into six groups (n = 7), namely: (1) Sham group, (2) Ast 100 mg/kg (Ast-H) group, (3) PM2.5 group, (4) Ast 50 mg/kg + PM2.5 (Ast-L + PM2.5) group, (5) Ast 100 mg/kg + PM2.5 (Ast-H + PM2.5) group, and (6) Ast 100 mg/kg + nigericin 4 mg/kg + PM2.5 (Ast-H+ Nig + PM2.5) group. Concretely, before the administration of PM2.5, except for the sham and PM2.5 groups, all other animals were injected intraperitoneally once daily for three days with Ast, which was dissolved in physiological saline containing 1‰ DMSO. Mice in the sham group and PM2.5 group were given with an equal volume of solvent by intraperitoneal injection. To evaluate the effect of Ast on NLRP3-mediated pyroptosis in PM2.5 caused lung toxicity, we administered nigericin to activate NLRP3. In the Ast-H + Nig + PM2.5 group, the mice were intraperitoneally injected with 100 mg/kg Ast 30 min after the intraperitoneal injection of nigericin. The dosage and mode of delivery of Ast and nigericin were based on previous researches [32,33]. Next, the PM2.5-induced model of lung toxicity was constructed through intratracheal instillation in accordance with the method previously reported [34,35]. All groups except the sham and Ast-H groups were intratracheally administered 7.5 mg/kg PM2.5 suspension (drip volume calculated at 1.5 ml/kg), which was repeated after 24 h. Mice were administrated the same volume of saline in the sham and Ast-H groups. The mice were sacrificed with sodium pentobarbital 12 h after the last intratracheal instillation [33]. Bronchoalveolar lavage fluid (BALF), as well as lung tissues were harvested and frozen in a −80 °C freezer for subsequent testing.

2.4. Survival analysis

To evaluate the therapeutic potential of Ast in mice exposed to PM2.5, we conducted a survival experiment as described previously, with minor modifications [36,37]. A further 42 mice were grouped and treated as above (n = 7). The day of PM2.5 exposure was defined as day 0. Then, the mortality rate of all mice was monitored and calculated for 10 days after PM2.5 exposure.

2.5. Wet weight to dry weight (W/D) ratio of lung tissue

The right middle lobe was isolated from mice, and the wet weight was measured. Subsequently, the removed right lung was baked in the oven for two days at 60 °C before measuring the dry weight. Lung edema was assessed by counting the W/D ratio of the lung.

2.6. Histopathological analysis

The right upper lung lobes were isolated and subsequently fixed with 4% paraformaldehyde for 24 h at room temperature, and next embedded in paraffin. Then, cutting the specimens into 4-μm-thick slices and staining it with hematoxylin and eosin (H&E). Histological observation was performed with microscope. To quantify the severity of lung toxicity by histology, the lung injury score was assessed as described previously [38,39].

2.7. Cytokines in BALF

BALF was obtained by intratracheal instillation of 1 ml saline twice in the left lung lobe and was centrifuged at 4 °C for 10 min at 1000*g*. The supernatants were harvested and reserved at −80 °C for later

measurement of cytokine concentrations, including TNF-α, IL-1β, IL-6, and IL-18 using ELISA kits in line with the manufacturer's recommendations.

2.8. Oxidative stress in the lung tissue

The concentrations of lung tissue MPO, MDA, and SOD of mice were determined using ELISA kits based on the manufacturer's instructions.

2.9. LDH release

The expressions level of LDH was measured in serum using an LDH release assay kit according with the manufacturer's recommendations.

2.10. Immunofluorescence staining

Cleaved caspase-1 immunofluorescence and co-localization of TUNEL double staining were used to detect cell pyroptosis. The fixation, embedding and cutting of lung samples agreed with the above the 2.6 histopathological analysis. After being dewaxed with xylene, the slices were processed with the TUNEL kit according to the manufacturer's instructions, followed by incubation overnight at 4 °C with anti-cleaved caspase-1 antibody (1:500). The next morning, at room temperature, the specimen was incubated with anti-rabbit immunoglobulin G (IgG)-labeled fluorescent secondary antibody (1:100) for 2 h. The nuclei were stained with 4',6-diamino-2-phenylindole (DAPI) for cellular localization. The slices were visualized with fluorescent microscope. The blue fluorescence (DAPI) reflects the nuclei, while the green and red fluorescence represent TUNEL-positive cells and caspase-1, respectively. The pyroptosis rate was calculated as the ratio of TUNEL-positive and cleaved caspase-1-positive co-localization to DAPI staining [40,41].

2.11. Western blot

After the extraction and quantification of total protein from the lung tissue, the equal number of protein samples were separated by 10% sodium dodecyl sulfate-polyacrylamide gel electrophoresis and transferred onto polyvinylidene fluoride (PVDF) membrane. Blocking buffer (5% skimmed milk or 5% bovine serum albumin) was employed to block the PVDF membrane at room temperature for 1 h, before applying the primary antibodies against the following targets: NLRP3 (1:1000), cleaved caspase-1 (1:1000), ASC2/ASC1 (1:5000), pro-caspase-1 (1:1000), cleaved IL-1β (1:1000), GSDMD (1:1000), cleaved GSDMD (1:1000), p65 (1:5000), p-p65 (1:5000), IκBα (1:5000), p-IκBα (1:5000), and GAPDH (1:10000). Membranes were separately incubated at 4 ℃ overnight. After washing three times with PBST, the secondary antibodies were used to incubate with membranes at room temperature for 2 h. Subsequently, protein bands were digitized and analyzed using a gel imaging system (BioRad, California, USA), and protein intensities were measured with Image J software (NIH, Bethesda, MD, USA).

2.12. Transmission electron microscopy (TEM)

The right lower lung lobe was fixed in glutaric dialdehyde solution for 24 h, washed with phosphate-buffered saline (PBS) 3 times, and then fixed with 1% osmium solution for 2 h. After the fixed solution was cleared, the samples were dehydrated with ethanol, soaked with acetone, embedded with acetone and 812, sliced with the uniform random sampling method, and stained with 2% dioxane acetate and lead citrate. Finally, the lung tissue ultrastructural structures were visualized by TEM (Hitachi, Japan).

2.13. Statistical analysis

Numerical values are given as mean ± standard error of the mean. All data analyses were processed using GraphPad Prism 8 (San Diego, CA, USA) via one-way analysis of variance followed by Tukey's *post-hoc* test. Survival curves are shown as Kaplan–Meier plots, and homogeneity was estimated by the log-rank test. Statistical significance was accepted when P value of < 0.05.

3. Results

3.1. Effect of Ast on the survival rate of mice exposed to PM2.5

As shown in Fig. 1A, the highest death rate of mice was recorded on the first day after modeling, and the survival rate was 70%. The first day survival rate both in the Ast-L + PM2.5 group and the Ast-H + PM2.5 group was about 83%. And it is in the Sham group and Ast-H group was 100%. However, on the 10th day, the survival rate of mice in the PM2.5 group decreased to 25% and was maintained until the animals were sacrificed. The survival rate in the Ast-L + PM2.5 group and the Ast-H + PM2.5 group was strikingly better than in the PM2.5 group. In parallel, nigericin counteracted the protective effect of Ast ($P < 0.05$). These results confirm that Ast might improve the survival rate of mice after PM2.5-caused lung toxicity via the NLRP3 inflammasome-related pathway.

3.2. Effect of Ast on PM2.5-caused lung toxicity in mice

As illustrated in Fig. 2A, the alveolar structures in the sham and Ast-H + PM2.5 groups were normal. In the PM2.5 group, alveolar hemorrhage, alveolar edema, septal thickening, and inflammatory cell infiltration were observed. Ast treatment remarkably ameliorated these pathological changes and reduced the pulmonary toxicity induced by PM2.5. Consistent with the trend in the histopathology results, lung injury score and W/D ratio substantially deteriorated after PM2.5 exposure, but they dramatically improved dose-dependently with Ast administration (Fig. 2B–C). However, nigericin counteracted the protective effect of Ast. These data indicate that Ast pre-treatment effectively attenuates PM2.5-induced lung toxicity in mice, and this protective role may be a result of NLRP3 inflammasome pathway inhibition.

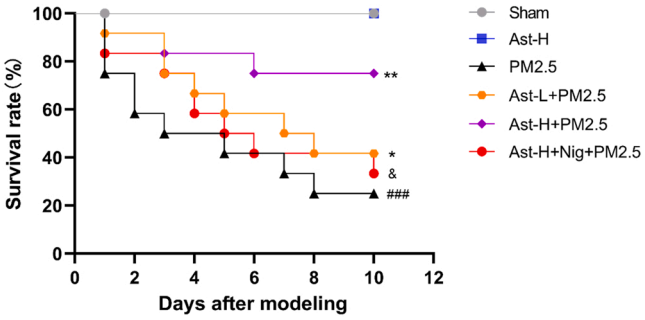

Fig. 1. Effect of Ast on survival rate of PM2.5-induced mice. The survival rates of mice were observed within 12d after PM2.5 challenge. Sham: control mice underwent a sham operation; Ast-H: Astragaloside IV (100 mg/kg) administered mice; PM2.5: PM2.5-induced lung toxicity mice; Ast-L+PM2.5: Astragaloside IV (50 mg/kg) pretreatment before PM2.5 intoxication; Ast-H+PM2.5: Astragaloside IV (100 mg/kg) pretreatment before PM2.5 intoxication; Ast-H+Nig+PM2.5: Astragaloside IV (100 mg/kg) in combination with Nigericin (the activator of NLRP3) before PM2.5 intoxication. Results are expressed as percent survival ($n = 7$). ###$P < 0.001$ compared with Sham group; *$P < 0.05$, and **$P < 0.01$, compared with PM2.5 group; &$P < 0.05$ compared with Ast-H+PM2.5 group. Survival curves are shown by Kaplan- Meier plots and the log-rank statistical test estimated their homogeneity.

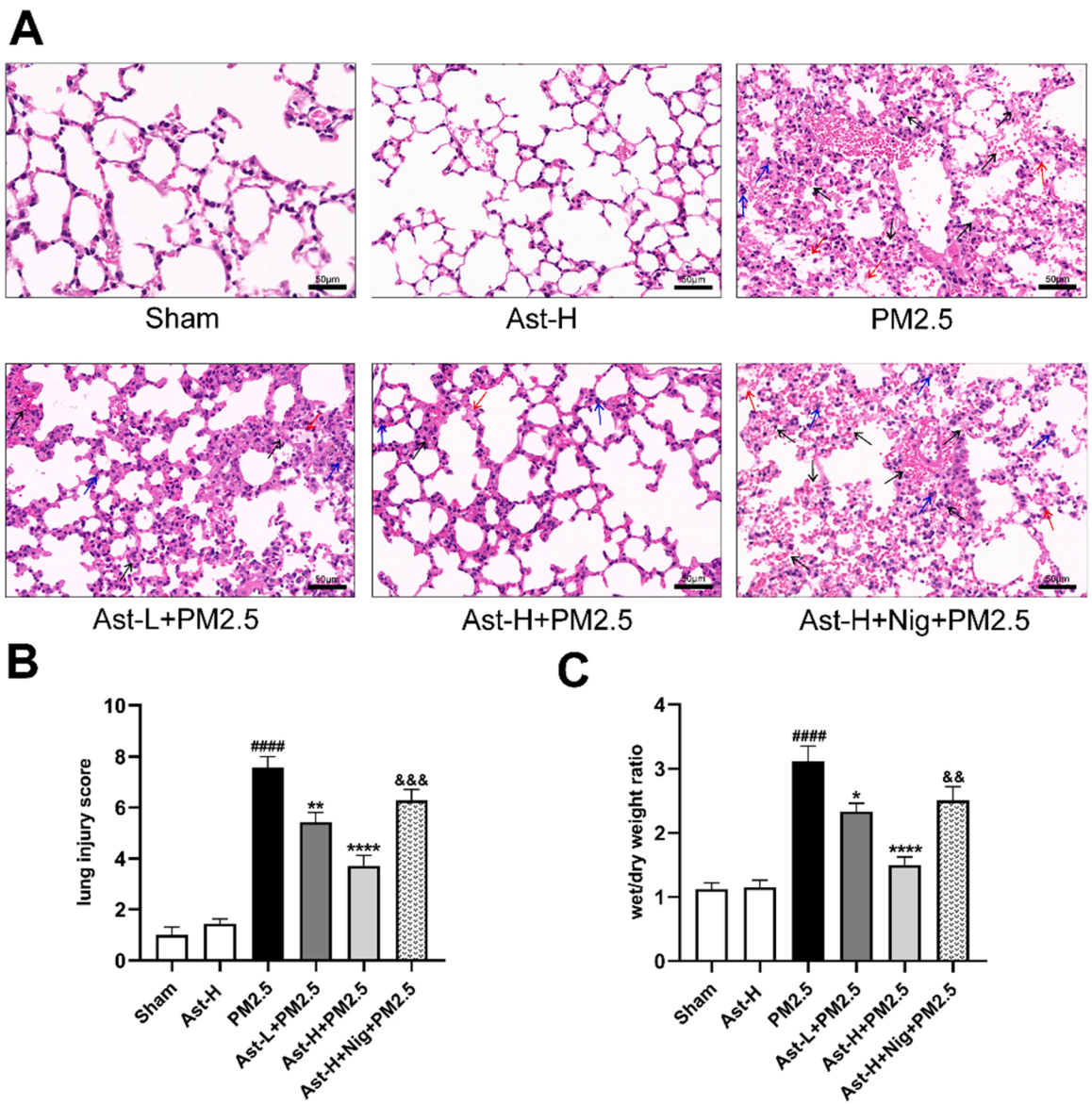

Fig. 2. Effect of Ast on PM2.5-induced lung toxicity in mice. (A) Ast protects lung histology during PM2.5-induced lung toxicity. Paraffin sections of lung tissues from Sham, Ast-H, PM2.5, Ast-L+PM2.5, Ast-H+PM2.5, and Ast-H+Nig+PM2.5 were stained with H&E staining (Magnification 100 ×, Scale bar = 100 μm). Black arrows: alveolar hemorrhage; Blue arrows: inflammatory cell infiltration; Red arrows: alveolar edema. (B) A semiquantitative histopathological score of lung injury. (C) Effect of Ast on lung wet/dry weight ratio of PM2.5-induced lung toxicity. Sham: control mice underwent a sham operation; Ast-H: Astragaloside IV (100 mg/kg) administered mice; PM2.5: PM2.5-induced lung toxicity mice; Ast-L+PM2.5: Astragaloside IV (50 mg/kg) pretreatment before PM2.5 intoxication; Ast-H+PM2.5: Astragaloside IV (100 mg/kg) pretreatment before PM2.5 intoxication; Ast-H+Nig+PM2.5: Astragaloside IV (100 mg/kg) in combination with Nigericin (the activator of NLRP3) before PM2.5 intoxication. Values are expressed as mean ± SEM (n = 7). All data were analyzed by one-way analysis of variance (ANOVA), followed by Tukey's post hoc test. ####P < 0.0001 compared with Sham group; *P < 0.05, and * *P < 0.01, compared with PM2.5 group; &P < 0.05 compared with Ast-H+PM2.5 group.

3.3. Effect of Ast on PM2.5-caused oxidative stress and lung toxicity in mice

PM2.5 caused an upregulation in MPO and MDA but a down-regulation in SOD. Ast restored the levels of MPO, MDA, and SOD in the lung tissue of PM2.5 exposure mice. Both doses of Ast significantly suppressed oxidative stress in mice exposed to PM2.5. While treatment with nigericin reversed the effects of Ast (Fig. 3), showing that Ast might act by blocking the NLRP3 inflammasome pathway.

3.4. Effect of Ast on inflammatory cytokine levels in mice with PM2.5-caused lung toxicity

Compared with the sham and Ast-H groups, elevated concentrations of TNF-α, IL-18, IL-1β, and IL-6 in BALF were observed in the PM2.5 group. Ast treatment markedly inhibited PM2.5-induced pro-inflammatory factor release in a dose- dependent manner, whereas nigericin reversed the Ast-induced changes in TNF-α, IL-18, IL-1β, and IL-6. These results suggest that Ast suppressed pro-inflammatory cytokine concentrations via inhibition of NLRP3 inflammasome activation (Fig. 4).

3.5. Effect of Ast on pyroptosis-related protein expression in mice with PM2.5-caused lung toxicity

To explore the effect of Ast on pyroptosis-related protein expression in mice with PM2.5-induced lung toxicity, we detected the concentrations of pyroptosis-related proteins by Western blotting. In Fig. 5, the levels of NLRP3, ASC, cleaved caspase-1/pro-caspase-1, GSGMD-N/

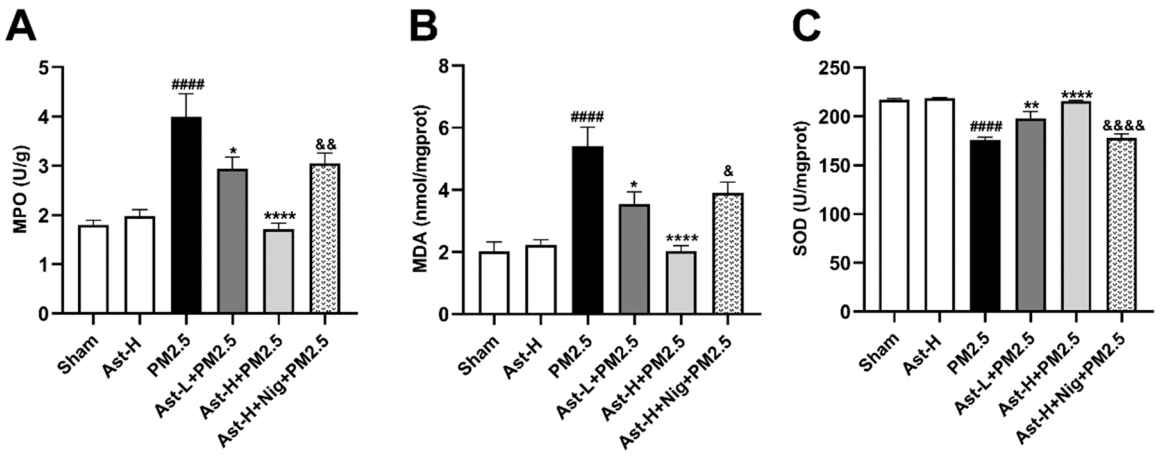

Fig. 3. Effect of Ast on oxidative stress of PM2.5-induced lung toxicity in mice. Effect of Ast on (A) MPO, (B) MDA, and (C) SOD in the lung tissue of PM2.5-induced mice. Sham: control mice underwent a sham operation; Ast-H: Astragaloside IV (100 mg/kg) administered mice; PM2.5: PM2.5-induced lung toxicity mice; Ast-L+PM2.5: Astragaloside IV (50 mg/kg) pretreatment before PM2.5 intoxication; Ast-H+PM2.5: Astragaloside IV (100 mg/kg) pretreatment before PM2.5 intoxication; Ast-H+Nig+PM2.5: Astragaloside IV (100 mg/kg) in combination with Nigericin (the activator of NLRP3) before PM2.5 intoxication. Values are expressed as mean ± SEM (n = 7). All data were analyzed by one-way analysis of variance (ANOVA), followed by Tukey's post hoc test. ####P < 0.0001 compared with Sham group; *P < 0.05, **P < 0.01, and *** *P < 0.0001 compared with PM2.5 group; &P < 0.05, &&P < 0.01, and &&&&P < 0.0001 compared with Ast-H+PM2.5 group.

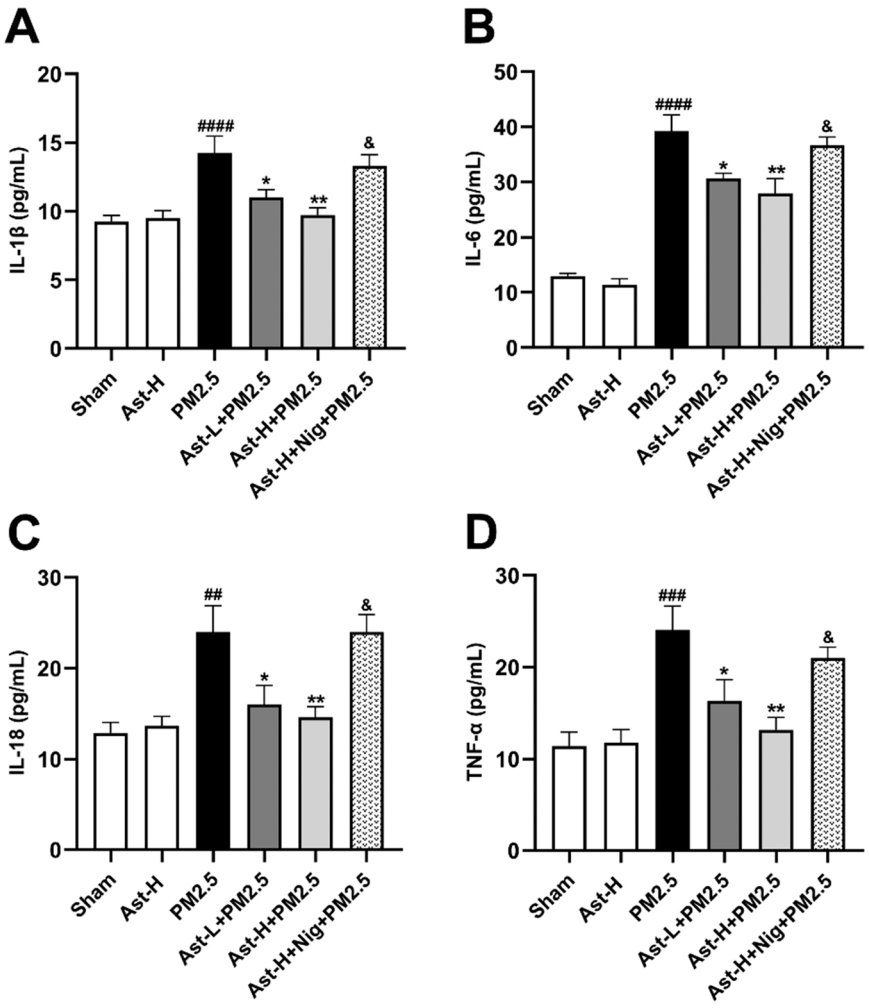

Fig. 4. Effects of Ast on inflammatory cytokine levels of PM2.5-induced lung toxicity in mice. Levels of (A) IL-1β, (B) IL-6, (C) IL-18, and (D) TNF-α in the BALF. Sham: control mice underwent a sham operation; Ast-H: Astragaloside IV (100 mg/kg) administered mice; PM2.5: PM2.5-induced lung toxicity mice; Ast-L+PM2.5: Astragaloside IV (50 mg/kg) pretreatment before PM2.5 intoxication; Ast-H+PM2.5: Astragaloside IV (100 mg/kg) pretreatment before PM2.5 intoxication; Ast-H+Nig+PM2.5: Astragaloside IV (100 mg/kg) in combination with Nigericin (the activator of NLRP3) before PM2.5 intoxication. Values are expressed as mean ± SEM (n = 7). ##P < 0.01, ###< 0.001, and ####P < 0.0001 compared with Sham group, *P < 0.05, and **P < 0.01 compared with PM2.5 group; &P < 0.05 compared with Ast-H+PM2.5 group.

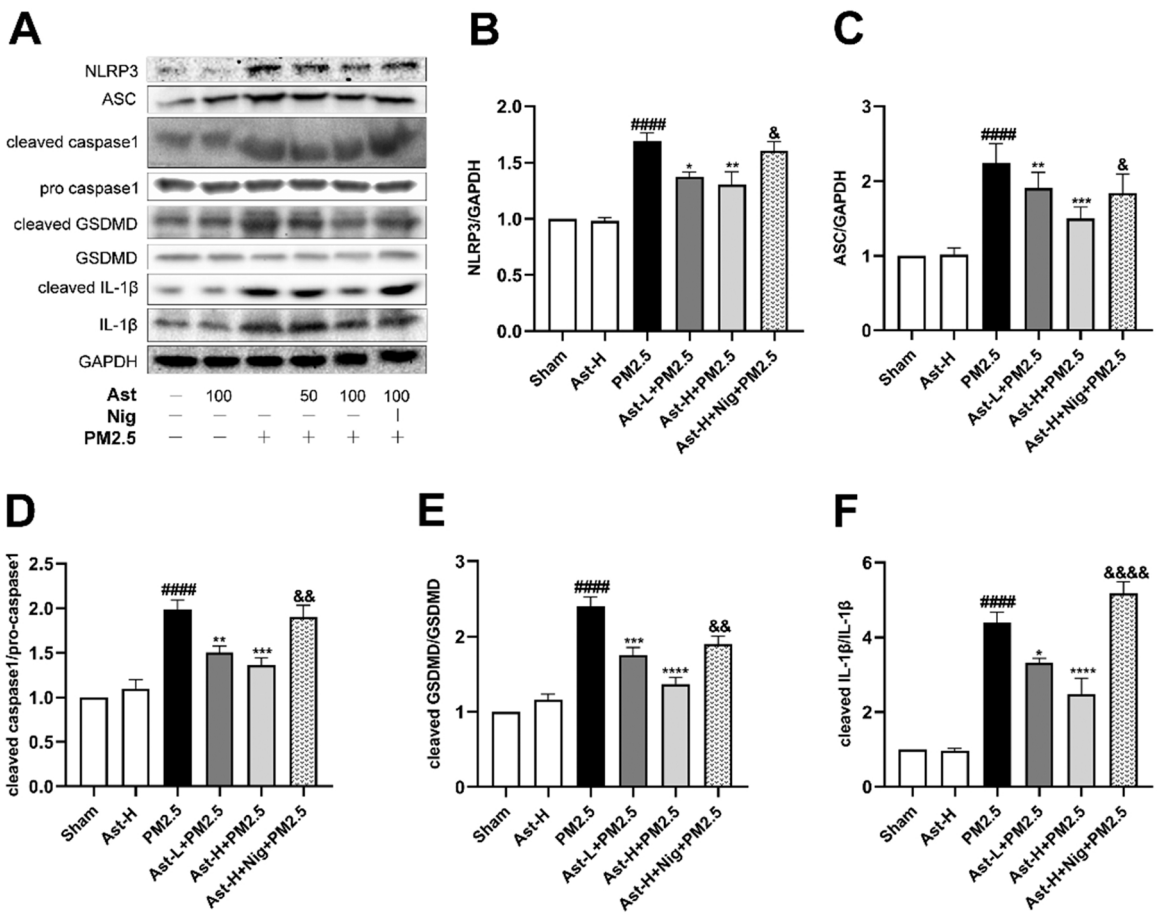

Fig. 5. Effects of Ast on the pyroptosis related proteins of PM2.5-induced lung toxicity in mice by Western blot. (A) Western blot analysis of the expression of pyroptosis related proteins in bladder. (B-F) Quantitative results of relative expressions of pyroptosis related proteins. Sham: control mice underwent a sham operation; Ast-H: Astragaloside IV (100 mg/kg) administered mice; PM2.5: PM2.5-induced lung toxicity mice; Ast-L+PM2.5: Astragaloside IV (50 mg/kg) pretreatment before PM2.5 intoxication; Ast-H+PM2.5: Astragaloside IV (100 mg/kg) pretreatment before PM2.5 intoxication; Ast-H+Nig+PM2.5: Astragaloside IV (100 mg/kg) in combination with Nigericin (the activator of NLRP3) before PM2.5 intoxication. All values were expressed as mean±SEM (n = 7). ####P < 0.0001 compared with Sham group; *P < 0.05, **P < 0.01, ***P < 0.001, and *** *P < 0.0001 compared with PM2.5 group; &P < 0.05, &&P < 0.01, and &&&&P < 0.0001 compared with Ast-H+PM2.5 group.

GSGMD, and cleaved IL-1β/IL-1β in the Ast-L+ PM2.5 and Ast-H + PM2.5 groups was markedly decreased compared with the PM2.5 group ($P < 0.05$). The relative expression of pyroptosis-related proteins was lower in the Ast-H + PM2.5 group than in the Ast-L+ PM2.5 group. Notably, these events were reversed by nigericin. Together, these results show that NLRP3 inflammasome-related pyroptosis is activated after PM2.5 exposure, and that Ast suppresses the expression of pyroptosis-related proteins via inhibition of NLRP3 inflammasome activation.

3.6. Ast alleviates NLRP3 inflammasome-mediated pyroptosis in mice with PM2.5-caused lung toxicity

To elucidate the impact of Ast on pyroptosis in mice with PM2.5-caused lung toxicity, we identified pyroptosis by immunofluorescence, LDH release, and TEM. The pyroptosis rates were calculated to identify pyroapoptotic cells in mice with PM2.5-caused lung toxicity. As shown in Fig. 6A–B, in the sham and Ast-H groups, pyroptotic cells were only rarely detected in lung tissues. Compared with the model group, Ast treatment reduced the percentage of pyroptotic cells. In agreement with these results, PM2.5 acutely increased LDH release, which is a hallmark of inflammasome-associated pyroptosis [42]. LDH release was dose-dependently inhibited by Ast. Moreover, in the PM2.5 group, alveolar macrophages with a typical pyroptotic morphology were also identified under TEM through the formation of holes on the cell membrane, which result in membrane integrity loss. Consistently, Ast restored the PM2.5-induced ultrastructural alterations of alveolar macrophages. Interestingly, nigericin reversed the changes induced by Ast. These results suggest that Ast might protect against PM2.5-resulted lung toxicity via suppressing NLRP3 inflammasome-mediated pyroptosis.

3.7. Effect of Ast on NF-κB signaling with PM2.5-caused lung toxicity in mice

As shown in Fig. 7, PM2.5 exposure caused a decrease in IκBα and p65 expression and a significant increase in phosphorylated IκBα and p65 expression, as detected by Western blotting. Ast strikingly decreased the expression of p-IκBα and p-p65 in a concentration-dependent manner. Importantly, the suppression of NF-κB signaling by Ast was blocked by nigericin. Taken together, the above findings indicate that Ast might inhibit NF-κB signaling via inhibition of NLRP3 inflammasome activation.

4. Discussion

Although multiple organs are affected, the lung is the main target organ of PM2.5 [43,44]. PM2.5-induced multiple cell death is strongly related to the pathogenesis of respiratory diseases. Previous research has convincingly illustrated that PM2.5-caused pulmonary toxicity is related to the activation of numerous cell death pathways, including autophagy [45], apoptosis [46], ferroptosis [47], and necrosis [48]. The regulation

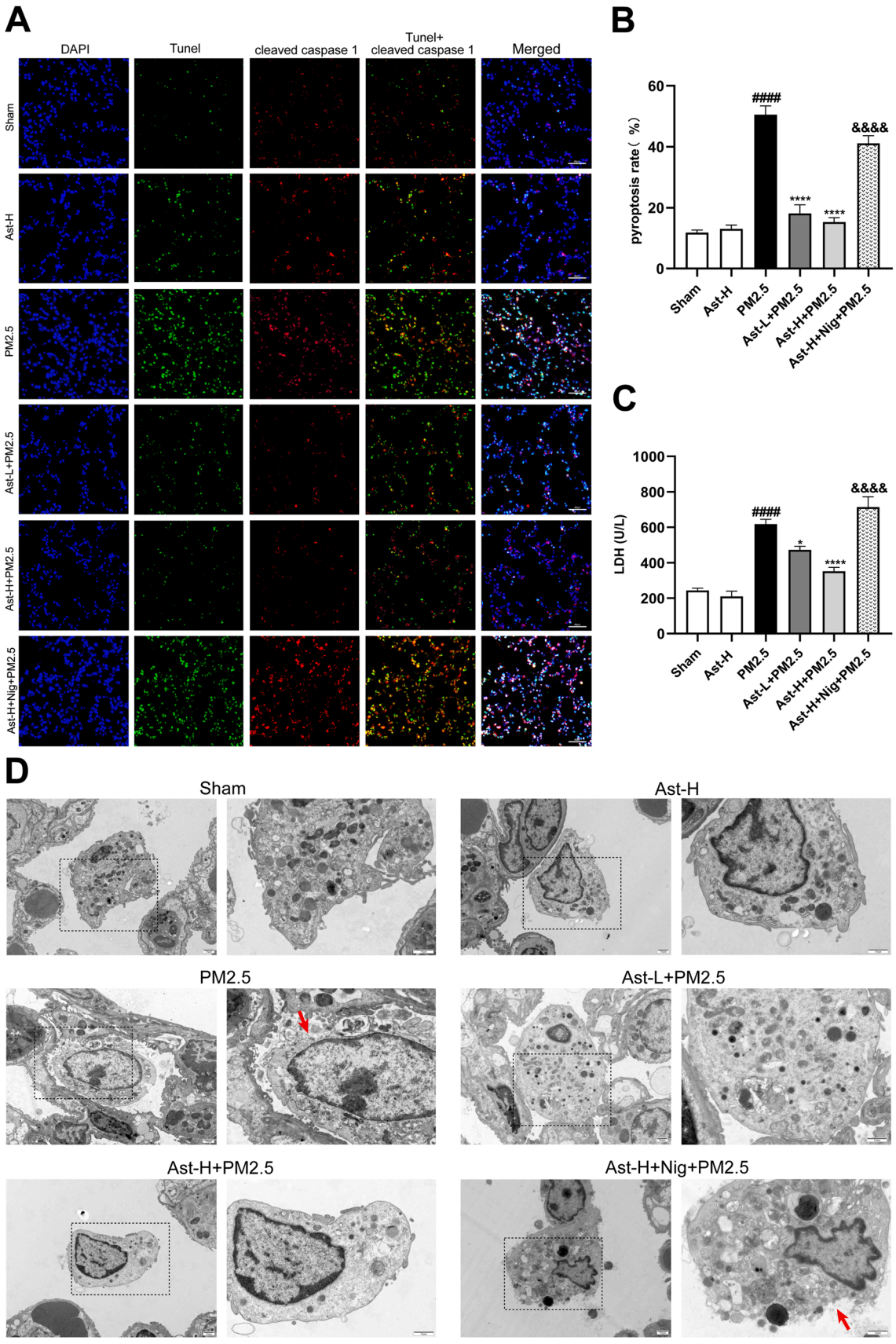

(caption on next page)

Fig. 6. Effect of Ast on the NLRP3 inflammasome-mediated pyroptosis of PM2.5-induced lung toxicity in mice. (A) Representative images of TUNEL and cleaved caspase-1 fluorescence double co-localization of lung sections from mice in all groups. (Magnification 200 ×, Scale bar = 40 μm). (B) Quantitation of pyroptosis rate. (C) LDH expression levels in the serum. (D) Representative images of TEM. Ultrastructure of alveolar macrophages undergoing pyroptosis was observed under the TEM. Red arrows indicate the pyroptotic cells with membrane pores, cytoplasmic swelling and nucleus pyknosis. (Magnification 2000 × for the left column and 5000 × for the right column, Scale bar = 10 μm). Sham: control mice underwent a sham operation; Ast-H: Astragaloside IV (100 mg/kg) administered mice; PM2.5: PM2.5-induced lung toxicity mice; Ast-L+PM2.5: Astragaloside IV (50 mg/kg) pretreatment before PM2.5 intoxication; Ast-H+PM2.5: Astragaloside IV (100 mg/kg) pretreatment before PM2.5 intoxication; Ast-H+Nig+PM2.5: Astragaloside IV (100 mg/kg) in combination with Nigericin (the activator of NLRP3) before PM2.5 intoxication. Data are expressed as mean ± SEM. ####P < 0.0001 compared with sham group; *P < 0.05 and ****P < 0.0001 compared with PM2.5 group; &&&&P < 0.0001 compared with Ast-H+PM2.5 group.

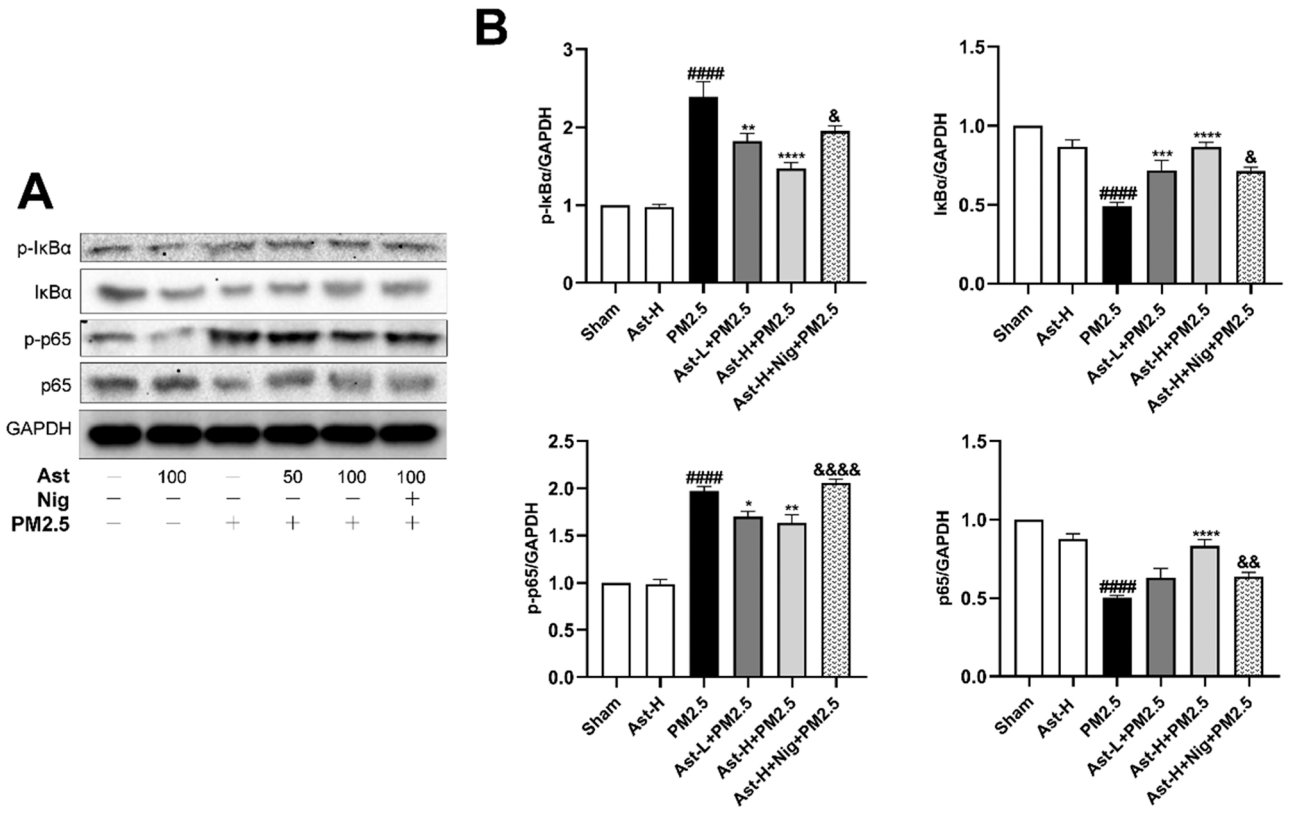

Fig. 7. Effect of Ast on NF-κB signaling of PM2.5-induced lung toxicity in mice by Western blot. (A) Western blot analysis of the expression of NF-κB proteins in the lung tissues. (B) Quantitative results of relative phosphorylation expressions of NF-κB proteins. Sham: control mice underwent a sham operation; Ast-H: Astragaloside IV (100 mg/kg) administered mice; PM2.5: PM2.5-induced lung toxicity mice; Ast-L+PM2.5: Astragaloside IV (50 mg/kg) pretreatment before PM2.5 intoxication; Ast-H+PM2.5: Astragaloside IV (100 mg/kg) pretreatment before PM2.5 intoxication; Ast-H+Nig+PM2.5: Astragaloside IV (100 mg/kg) in combination with Nigericin (the activator of NLRP3) before PM2.5 intoxication. All values are expressed as mean ± SEM (n = 7). ####P < 0.0001 compared with Sham group; *P < 0.05, **P < 0.01, ***P < 0.001, and ****P < 0.0001 compared with PM2.5 group; &P < 0.05, &&P < 0.01, and &&&&P < 0.0001 compared with Ast-H+PM2.5 group.

of these cell-fate decisions is likely the main control tactic against PM2.5-caused lung injury [49]. However, to date, no clinical agents are available for both prevention and treatment of PM2.5-caused toxicity in the lung. In this research, we demonstrated that PM2.5 led to hemorrhage in lung tissues, obvious alveolar congestion, alveolar wall thickening, an increase in erythrocytes in the alveolar cavity and pulmonary interstitium, and neutrophil infiltration in the alveolar cavity and blood vessel walls. Ast protected against PM2.5- caused lung toxicity via downregulating inflammasome-mediated pyroptosis through inhibition of NLRP3/caspase-1 signaling, resulting in prolonged survival in mice. Pre-administration of Ast may protect mice from PM2.5-induced pulmonary toxicity through this mechanism.

Mounting evidence shows that PM2.5-induced pulmonary toxicity is manifested by increased oxidative stress injury and a variety of pro-inflammatory cytokines [50,51]. Furthermore, reactive oxygen species may further induce the production of pro-inflammatory cytokines, increasing cellular oxidative stress [52]. Previous researches have illustrated that PM2.5-caused lung injury can be alleviated by suppressing pro-inflammatory cytokines and oxidative stress [25,53]. Similarly, in our study, Ast markedly inhibited the concentrations of TNF-α, IL-1β, IL-18, and IL-6 in BALF. Consistently, Ast can also inhibit oxidative stress. NF-κB is a major regulator of oxidative stress and inflammation [54,55]. In this study, the increased levels of oxidative stress and inflammation further contributed to activation of NF-κB. Multiple studies have established that the suppression of NF-κB attenuated the levels of inflammation and oxidative stress [56,57]. Furthermore, Ast also significantly inhibited the NF-κB pathway, which is agreement with conclusion of our earlier study [25,33]. The potential anti-inflammatory property of Ast might partly explain the beneficial mechanism of its protection against PM2.5-caused lung tissue injury. Thus, the present results are in accordance with previous findings that Ast exerts anti-inflammatory effects via various pathways, including Adenosine Monophosphate Activated Protein Kinase [35], c-Jun N-terminal kinase, Nuclear factor E2-related factor 2 [58], and Extracellular signal-regulated kinase [59]. Notably, recent researches have indicated that the reactive oxygen species generation and NF-κB activation are

known to trigger NLRP3-mediated pyroptosis in inflammatory diseases [60–62]. Therefore, we deduce that Ast may protect against PM2.5-caused lung toxicity via regulating the NLRP3-mediated pyroptosis pathway.

In the classic pathway of NLRP3 inflammation, activation of the NF-κB pathway initiates NLRP3 activation [63,64]. After further assembly, cleaved caspase-1 and IL-1β promotes the maturation of IL-1β, thereby amplifying the inflammatory response [65,66]. Previous studies have confirmed that the NLRP3 inflammasome serves an important contributor in various inflammatory diseases attacked by PM2.5 exposure [23,67]. Thus, we addressed the impact of Ast on the NF-κB/NLRP3 axis in PM2.5-caused lung toxicity. In our results, PM2.5 resulted the phosphorylation of NF-κB p65, which is considered necessary for the NLRP3 inflammasome activation. Ast dramatically downregulated the concentration of NF-κB, NLRP3, and IL-1β in lung tissues from mice. Meanwhile, these events were reversed by nigericin (an NLRP3 activator), indicating that Ast might attenuate PM2.5-induced lung toxicity through inhibition of NLRP3 signaling. Several literatures have reported that Ast may exert a protective role in multiple inflammatory models by regulating the NLRP3 inflammasome [22,68]. However, the mechanism of Ast on NLPR3 requires further study.

In recent years, the NLRP3 inflammasome has been confirmed to exert a major role in the pathogenesis of respiratory disorders [69]. The NLRP3 inflammasome is typically comprised of an NLRP3 inflammasome sensor, ASC, and pro-caspase-1 [70]. NLRP3 inflammasome activation is closely associated with inflammation and pyroptosis [71]. In the classical process of pyroptosis, NLRP3 inflammasome activation account for the caspase-1 activation, which initiates the cleavage of pro-IL-1β, pro-IL-18, and GSDMD [72]. Thereafter, caspase-1 cleaves GSDMD, resulting in pore formation on the cell membrane and causing the release and secretion of IL-1β, IL-18, and LDH [73,74]. As a lytic type of cell death, pyroptosis has not been extensively studied in PM2.5-induced respiratory diseases [31]. Several recent studies also suggested that PM2.5 increases pyroptosis in the damage of lung, but no pyroptotic cells have been directly observed in vivo [23,26]. Here, PM2.5 observably risen pyroptosis-associated protein expression and LDH release, leading to activation of the inflammatory cascade. Importantly, TEM showed that alveolar macrophages are the main pyroptotic cells in PM2.5-caused lung toxicity. In agreement to this result, other study suggested that NLRP3-mediated macrophage pyroptosis induces inflammation, as well as oxidative stress in PM2.5-caused damage of lung [26]. Moreover, there are currently no clinical inhibitors that target NLRP3 to prevent PM2.5-induced lung toxicity, although several studies have indicated that NLRP3 inhibition may attenuate PM2.5 resulted respiratory injury [26,67]. In our study, we not only found that Ast reduces pyroptosis and inflammation by inhibiting the NLRP3/caspase-1/GSDMD axis, but it also protects the ultrastructure of alveolar macrophages. Nevertheless, nigericin reverses the changes induced by Ast, which illustrates that Ast protects against PM2.5-caused lung toxicity through suppressing NLRP3 inflammasome-mediated pyroptosis. Similar to the present results, previous research found that pre-treatment with MCC950, which is a specific NLRP3 inhibitor, protects from PM2.5-caused pulmonary inflammation in mice [23]. As shown in the Fig. 8, these findings indicate that Ast protects against PM2.5 caused lung toxicity by suppressing inflammasome-mediated pyroptosis via NLRP3/caspase-1 axis inhibition. Thus, targeting the NLRP3 inflammasome might be a very promising control strategy against PM2.5-induced respiratory injury. The specific mechanisms, however, require to be further inquired.

5. Conclusion

In conclusion, our findings illustrate that Ast protects against PM2.5-induced lung toxicity by suppressing inflammasome-mediated pyroptosis via NLRP3/caspase-1 axis inhibition in mice, thereby protecting the lung against PM2.5-caused pulmonary inflammation and oxidative damage. The present study provides new insights into the therapeutic potential of Ast, suggesting that it may be a promising candidate for the prevention of PM2.5-caused respiratory disorders. Targeting the NLRP3 inflammasome might be a novel promising strategy for PM2.5 caused respiratory injury.

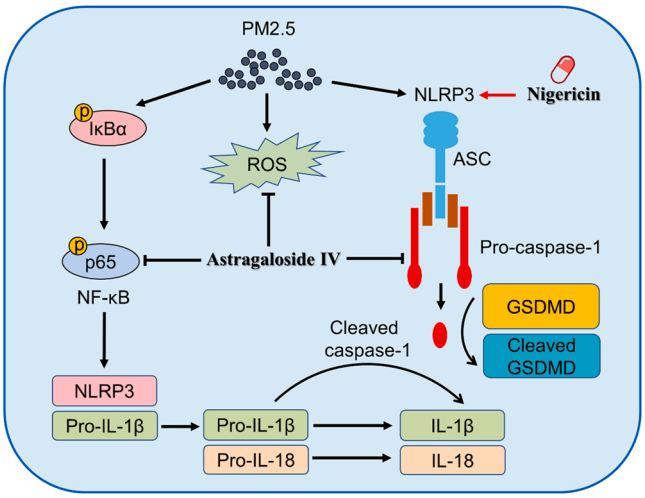

Fig. 8. Underlying mechanisms of the protective effect of Ast against PM2.5-induced lung toxicity in mice. On the one hand, PM2.5 induced oxidative stress and caused to the activation of both NF-κB and NLRP3, resulting the initiation of NLRP3 inflammasome. Subsequently, the phosphorylation and activation of NF-κB increased the amounts of NLRP3 as well as initiated synthesis of pro-IL-1β. In addition, caspase-1-dependent pro-IL-1β, pro-IL-18 and GSDMD cleavage and secretion of their bioactive forms: IL-1β and IL-18, cleaved-GSDMD, resulting the dramatic inflammatory response. Ast, on other hand, has a protective effect on the PM2.5-induced pulmonary toxicity by suppressing inflammasome-mediated pyroptosis via inhibiting the NLRP3/caspase-1 axis, thereby protecting the lung against PM2.5-induced lung inflammation and oxidative damage.

CRediT authorship contribution statement

Demei Huang: Writing – original draft. **Shihua Shi:** Writing – original draft. **Yilan Wang:** Data curation, Software. **Xiaomin Wang:** Data curation, Software. **Zherui Shen:** Experimentation. **Mingjie Wang:** Experimentation. **Caixia Pei:** Methodology. **Yongcan Wu:** Methodology. **Yacong He:** Visualization, Investigation, Supervision, Conceptualization, Writing – review & editing. **Zhenxing Wang:** Supervision, Conceptualization, Writing – review & editing. All authors reviewed and approved the final manuscript.

Conflict of interest statement

We declare that we have no known competing financial interests or personal relationships that could have appeared to influence the work reported in this paper.

Acknowledgments

This study was financially supported by the National Natural Science Foundation of China (No. 82104824), China Postdoctoral Science Foundation (No. 2020M683645XB), and the Key R&D Program of Sichuan Provincial Department of Science and Technology (No. 2020YFS0312).

Appendix A. Supplementary material

Supplementary data associated with this article can be found in the online version at doi:10.1016/j.biopha.2022.112978.

References

[1] A.J. Cohen, M. Brauer, R. Burnett, H.R. Anderson, J. Frostad, K. Estep, K. Balakrishnan, B. Brunekreef, L. Dandona, R. Dandona, V. Feigin, G. Freedman, B. Hubbell, A. Jobling, H. Kan, L. Knibbs, Y. Liu, R. Martin, L. Morawska, C. A. Pope 3rd, H. Shin, K. Straif, G. Shaddick, M. Thomas, R. van Dingenen, A. van Donkelaar, T. Vos, C.J.L. Murray, M.H. Forouzanfar, Estimates and 25-year trends of the global burden of disease attributable to ambient air pollution: an analysis of data from the Global Burden of Diseases Study 2015, Lancet 389 (10082) (2017) 1907–1918.

[2] C. Liu, R. Chen, F. Sera, A.M. Vicedo-Cabrera, Y. Guo, S. Tong, M. Coelho, P.H. N. Saldiva, E. Lavigne, P. Matus, N. Valdes Ortega, S. Osorio Garcia, M. Pascal, M. Stafoggia, M. Scortichini, M. Hashizume, Y. Honda, M. Hurtado-Díaz, J. Cruz, B. Nunes, J.P. Teixeira, H. Kim, A. Tobias, C. Íñiguez, B. Forsberg, C. Åström, M. S. Ragettli, Y.L. Guo, B.Y. Chen, M.L. Bell, C.Y. Wright, N. Scovronick, R. M. Garland, A. Milojevic, J. Kyselý, A. Urban, H. Orru, E. Indermitte, J.J. K. Jaakkola, N.R.I. Ryti, K. Katsouyanni, A. Analitis, A. Zanobetti, J. Schwartz, J. Chen, T. Wu, A. Cohen, A. Gasparrini, H. Kan, Ambient particulate air pollution and daily mortality in 652 cities, N. Engl. J. Med. 381 (8) (2019) 705–715.

[3] C.J. Obot, M.T. Morandi, R.F. Hamilton, A. Holian, A comparison of murine and human alveolar macrophage responses to urban particulate matter, Inhal. Toxicol. 16 (2) (2004) 69–76.

[4] E. Longhin, E. Pezzolato, P. Mantecca, J.A. Holme, A. Franzetti, M. Camatini, M. Gualtieri, Season linked responses to fine and quasi-ultrafine Milan PM in cultured cells, Toxicol. Vitr. 27 (2) (2013) 551–559.

[5] X. Xu, H. Wang, S. Liu, C. Xing, Y. Liu, Aodengqimuge, W. Zhou, X. Yuan, Y. Ma, M. Hu, Y. Hu, S. Zou, Y. Gu, S. Peng, S. Yuan, W. Li, Y. Ma, L. Song, TP53-dependent autophagy links the ATR-CHEK1 axis activation to proinflammatory VEGFA production in human bronchial epithelial cells exposed to fine particulate matter (PM2.5), Autophagy 12 (10) (2016) 1832–1848.

[6] G. Wang, L. Huang, S. Gao, S. Gao, L. Wang, Measurements of PM10 and PM2.5 in urban area of Nanjing, China and the assessment of pulmonary deposition of particle mass, Chemosphere 48 (7) (2002) 689–695.

[7] L. Li, C. Xing, J. Zhou, L. Niu, B. Luo, M. Song, J. Niu, Y. Ruan, X. Sun, Y. Lei, Airborne particulate matter (PM(2.5)) triggers ocular hypertension and glaucoma through pyroptosis, Part. Fibre Toxicol. 18 (1) (2021) 10.

[8] Y.F. Xing, Y.H. Xu, M.H. Shi, Y.X. Lian, The impact of PM2.5 on the human respiratory system, J. Thorac. Dis. 8 (1) (2016) E69–E74.

[9] B.T. Cookson, M.A. Brennan, Pro-inflammatory programmed cell death, Trends Microbiol. 9 (3) (2001) 113–114.

[10] S.L. Fink, B.T. Cookson, Caspase-1-dependent pore formation during pyroptosis leads to osmotic lysis of infected host macrophages, Cell. Microbiol. 8 (11) (2006) 1812–1825.

[11] E.I. Elliott, F.S. Sutterwala, Initiation and perpetuation of NLRP3 inflammasome activation and assembly, Immunol. Rev. 265 (1) (2015) 35–52.

[12] F. Martinon, A. Mayor, J. Tschopp, The inflammasomes: guardians of the body, Annu. Rev. Immunol. 27 (2009) 229–265.

[13] F.S. Sutterwala, Y. Ogura, D.S. Zamboni, C.R. Roy, R.A. Flavell, NALP3: a key player in caspase-1 activation, J. Endotoxin Res. 12 (4) (2006) 251–256.

[14] J. Shi, Y. Zhao, K. Wang, X. Shi, Y. Wang, H. Huang, Y. Zhuang, T. Cai, F. Wang, F. Shao, Cleavage of GSDMD by inflammatory caspases determines pyroptotic cell death, Nature 526 (7575) (2015) 660–665.

[15] L. Ning, W. Wei, J. Wenyang, X. Rui, G. Qing, Cytosolic DNA-STING-NLRP3 axis is involved in murine acute lung injury induced by lipopolysaccharide, Clin. Transl. Med. 10 (7) (2020), e228.

[16] S. Xiong, Z. Hong, L.S. Huang, Y. Tsukasaki, S. Nepal, A. Di, M. Zhong, W. Wu, Z. Ye, X. Gao, G.N. Rao, D. Mehta, J. Rehman, A.B. Malik, IL-1β suppression of VE-cadherin transcription underlies sepsis-induced inflammatory lung injury, J. Clin. Investig. 130 (7) (2020) 3684–3698.

[17] Z. Zasłona, E. Flis, M.M. Wilk, R.G. Carroll, E.M. Palsson-McDermott, M.M. Hughes, C. Diskin, K. Banahan, D.G. Ryan, A. Hooftman, A. Misiak, J. Kearney, G. Lochnit, W. Bertrams, T. Greulich, B. Schmeck, O.J. McElvaney, K.H.G. Mills, E.C. Lavelle, M. Wygrecka, E.M. Creagh, L.A.J. O'Neill, Caspase-11 promotes allergic airway inflammation, Nat. Commun. 11 (1) (2020) 1055.

[18] M. Zhang, Q. He, G. Chen, P.A. Li, Suppression of NLRP3 inflammasome, pyroptosis, and cell death by NIM811 in rotenone-exposed cells as an in vitro model of Parkinson's disease, Neurodegener. Dis. 20 (2–3) (2020) 73–83.

[19] Q. Zhao, C. Hao, J. Wei, R. Huang, C. Li, W. Yao, Bone marrow-derived mesenchymal stem cells attenuate silica-induced pulmonary fibrosis by inhibiting apoptosis and pyroptosis but not autophagy in rats, Ecotoxicol. Environ. Saf. 216 (2021), 112181.

[20] Q. Liang, W. Cai, Y. Zhao, H. Xu, H. Tang, D. Chen, F. Qian, L. Sun, Lycorine ameliorates bleomycin-induced pulmonary fibrosis via inhibiting NLRP3 inflammasome activation and pyroptosis, Pharmacol. Res. 158 (2020), 104884.

[21] J.F. Teng, Q.B. Mei, X.G. Zhou, Y. Tang, R. Xiong, W.Q. Qiu, R. Pan, B.Y. Law, V. K. Wong, C.L. Yu, H.A. Long, X.L. Xiao, F. Zhang, J.M. Wu, D.L. Qin, A.G. Wu, Polyphyllin VI induces caspase-1-mediated pyroptosis via the induction of ROS/NF-κB/NLRP3/GSDMD signal axis in non-small cell lung cancer, Cancers 12 (1) (2020).

[22] R. Zhang, X. Zhang, B. Xing, J. Zhao, P. Zhang, D. Shi, F. Yang, Astragaloside IV attenuates gestational diabetes mellitus via targeting NLRP3 inflammasome in genetic mice, Reprod. Biol. Endocrinol. 17 (1) (2019) 77.

[23] H. Jia, Y. Liu, D. Guo, W. He, L. Zhao, S. Xia, PM2.5-induced pulmonary inflammation via activating of the NLRP3/caspase-1 signaling pathway, Environ. Toxicol. 36 (3) (2021) 298–307.

[24] M. Sayan, B.T. Mossman, The NLRP3 inflammasome in pathogenic particle and fibre-associated lung inflammation and diseases, Part. Fibre Toxicol. 13 (1) (2016) 51.

[25] Y. Wu, W. Xiao, C. Pei, M. Wang, X. Wang, D. Huang, F. Wang, Z. Wang, Astragaloside IV alleviates PM2.5-induced lung injury in rats by modulating TLR4/MyD88/NF-κB signalling pathway, Int. Immunopharmacol. 91 (2021), 107290.

[26] R. Xiong, W. Jiang, N. Li, B. Liu, R. He, B. Wang, Q. Geng, PM2.5-induced lung injury is attenuated in macrophage-specific NLRP3 deficient mice, Ecotoxicol. Environ. Saf. 221 (2021), 112433.

[27] K.K. Auyeung, Q.B. Han, J.K. Ko, Astragalus membranaceus: a review of its protection against inflammation and gastrointestinal cancers, Am. J. Chin. Med. 44 (1) (2016) 1–22.

[28] P. Liu, H. Zhao, Y. Luo, Anti-aging implications of Astragalus membranaceus (Huangqi): a well-known chinese tonic, Aging Dis. 8 (6) (2017) 868–886.

[29] J. Zhang, C. Wu, L. Gao, G. Du, X. Qin, Astragaloside IV derived from Astragalus membranaceus: a research review on the pharmacological effects, Adv. Pharmacol. 87 (2020) 89–112.

[30] B. Leng, Y. Zhang, X. Liu, Z. Zhang, Y. Liu, H. Wang, M. Lu, Astragaloside IV suppresses high glucose-induced NLRP3 inflammasome activation by inhibiting TLR4/NF-κB and CaSR, Mediat. Inflamm. 2019 (2019), 1082497.

[31] Y. Wang, Y. Zhong, J. Liao, G. Wang, PM2.5-related cell death patterns, Int. J. Med. Sci. 18 (4) (2021) 1024–1029.

[32] C.C. Deng, Y. Liang, M.S. Wu, F.T. Feng, W.R. Hu, L.Z. Chen, Q.S. Feng, J.X. Bei, Y. X. Zeng, Nigericin selectively targets cancer stem cells in nasopharyngeal carcinoma, Int. J. Biochem. Cell Biol. 45 (9) (2013) 1997–2006.

[33] C. Pei, F. Wang, D. Huang, S. Shi, X. Wang, Y. Wang, S. Li, Y. Wu, Z. Wang, Astragaloside IV protects from PM2.5-induced lung injury by regulating autophagy via inhibition of PI3K/Akt/mTOR signaling in vivo and in vitro, J. Inflamm. Res. 14 (2021) 4707–4721.

[34] Z.H. Chen, Y.F. Wu, P.L. Wang, Y.P. Wu, Z.Y. Li, Y. Zhao, J.S. Zhou, C. Zhu, C. Cao, Y.Y. Mao, F. Xu, B.B. Wang, S.A. Cormier, S.M. Ying, W. Li, H.H. Shen, Autophagy is essential for ultrafine particle-induced inflammation and mucus hyperproduction in airway epithelium, Autophagy 12 (2) (2016) 297–311.

[35] F. Xu, W.Q. Cui, Y. Wei, J. Cui, J. Qiu, L.L. Hu, W.Y. Gong, J.C. Dong, B.J. Liu, Astragaloside IV inhibits lung cancer progression and metastasis by modulating macrophage polarization through AMPK signaling, J. Exp. Clin. Cancer Res. 37 (1) (2018) 207.

[36] A. Ayala, C.S. Chung, J.L. Lomas, G.Y. Song, L.A. Doughty, S.H. Gregory, W. G. Cioffi, B.W. LeBlanc, J. Reichner, H.H. Simms, P.S. Grutkoski, Shock-induced neutrophil mediated priming for acute lung injury in mice: divergent effects of TLR-4 and TLR-4/FasL deficiency, Am. J. Pathol. 161 (6) (2002) 2283–2294.

[37] T. Cheng, J. Bai, C.S. Chung, Y. Chen, E.A. Fallon, A. Ayala, Herpes virus entry mediator (HVEM) expression promotes inflammation/organ injury in response to experimental indirect-acute lung injury, Shock 51 (4) (2019) 487–494.

[38] C.E. D'Negri, E.L. De, Vito, Making it possible to measure knowledge, experience and intuition in diagnosing lung injury severity: a fuzzy logic vision based on the Murray score, BMC Med. Inf. Decis. Mak. 10 (2010) 70.

[39] R.M. McGuigan, P. Mullenix, L.L. Norlund, D. Ward, M. Walts, K. Azarow, Acute lung injury using oleic acid in the laboratory rat: establishment of a working model and evidence against free radicals in the acute phase, Curr. Surg. 60 (4) (2003) 412–417.

[40] Y. She, L. Shao, Y. Zhang, Y. Hao, Y. Cai, Z. Cheng, C. Deng, X. Liu, Neuroprotective effect of glycosides in Buyang Huanwu Decoction on pyroptosis following cerebral ischemia-reperfusion injury in rats, J. Ethnopharmacol. 242 (2019), 112051.

[41] Z. Zhang, R. Ricci, Hijacking the NLRP3 inflammasome: a mechanism underlying viral respiratory disease? EMBO Rep. 21 (7) (2020), e50645.

[42] M. Rayamajhi, Y. Zhang, E.A. Miao, Detection of pyroptosis by measuring released lactate dehydrogenase activity, Methods Mol. Biol. 1040 (2013) 85–90.

[43] R. Li, R. Zhou, J. Zhang, Function of PM2.5 in the pathogenesis of lung cancer and chronic airway inflammatory diseases, Oncol. Lett. 15 (5) (2018) 7506–7514.

[44] M. Riediker, D. Zink, W. Kreyling, G. Oberdörster, A. Elder, U. Graham, I. Lynch, A. Duschl, G. Ichihara, S. Ichihara, T. Kobayashi, N. Hisanaga, M. Umezawa, T. J. Cheng, R. Handy, M. Gulumian, S. Tinkle, F. Cassee, Particle toxicology and health - where are we? Part. Fibre Toxicol. 16 (1) (2019) 19.

[45] X.M. Zhu, Q. Wang, W.W. Xing, M.H. Long, W.L. Fu, W.R. Xia, C. Jin, N. Guo, D. Q. Xu, D.G. Xu, PM2.5 induces autophagy-mediated cell death via NOS2 signaling in human bronchial epithelium cells, Int. J. Biol. Sci. 14 (5) (2018) 557–564.

[46] X. Han, Y. Zhuang, PM2.5 induces autophagy-mediated cell apoptosis via PI3K/AKT/mTOR signaling pathway in mice bronchial epithelium cells, Exp. Ther. Med. 21 (1) (2021) 1.

[47] Y. Wang, M. Tang, PM2.5 induces ferroptosis in human endothelial cells through iron overload and redox imbalance, Environ. Pollut. 254 (Pt. A) (2019), 112937.

[48] W. Zhou, X. Yuan, L. Zhang, B. Su, D. Tian, Y. Li, J. Zhao, Y. Wang, S. Peng, Overexpression of HO-1 assisted PM2.5-induced apoptosis failure and autophagy-related cell necrosis, Ecotoxicol. Environ. Saf. 145 (2017) 605–614.

[49] S. Feng, D. Gao, F. Liao, F. Zhou, X. Wang, The health effects of ambient PM2.5 and potential mechanisms, Ecotoxicol. Environ. Saf. 128 (2016) 67–74.

[50] Q.Y. Ma, D.Y. Huang, H.J. Zhang, S. Wang, X.F. Chen, Exposure to particulate matter 2.5 (PM2.5) induced macrophage-dependent inflammation, characterized by increased Th1/Th17 cytokine secretion and cytotoxicity, Int. Immunopharmacol. 50 (2017) 139–145.

[51] S.A. Weichenthal, K. Godri-Pollitt, P.J. Villeneuve, PM2.5, oxidant defence and cardiorespiratory health: a review, Environ. Health 12 (2013) 40.

[52] Z.W. Zhang, X.C. Xu, T. Liu, S. Yuan, Mitochondrion-permeable antioxidants to treat ROS-burst-mediated acute diseases, Oxid. Med. Cell. Longev. 2016 (2016), 6859523.

[53] H. Zhang, L. Xue, B. Li, H. Tian, Z. Zhang, S. Tao, Therapeutic potential of bixin in PM2.5 particles-induced lung injury in an Nrf2-dependent manner, Free Radic. Biol. Med. 126 (2018) 166–176.
[54] M.S. Hayden, S. Ghosh, Shared principles in NF-kappaB signaling, Cell 132 (3) (2008) 344–362.
[55] A. Oeckinghaus, M.S. Hayden, S. Ghosh, Crosstalk in NF-κB signaling pathways, Nat. Immunol. 12 (8) (2011) 695–708.
[56] B. Hoesel, J.A. Schmid, The complexity of NF-κB signaling in inflammation and cancer, Mol. Cancer 12 (2013) 86.
[57] T. Liu, L. Zhang, D. Joo, S.C. Sun, NF-κB signaling in inflammation, Signal Transduct. Target. Ther. 2 (2017) 17023.
[58] F. Wang, S. Chen, L. Deng, L. Chen, Y. Huang, M. Tian, C. Li, X. Zhou, Protective effects of astragaloside IV against LPS-induced endometritis in mice through inhibiting activation of the NF-κB, p38 and JNK signaling pathways, Molecules 24 (2) (2019).
[59] L. Li, W. Huang, S. Wang, K. Sun, W. Zhang, Y. Ding, L. Zhang, B. Tumen, L. Ji, C. Liu, Astragaloside IV attenuates acetaminophen-induced liver injuries in mice by activating the Nrf2 signaling pathway, Molecules 23 (8) (2018).
[60] J. Cai, H. Guan, X. Jiao, J. Yang, X. Chen, H. Zhang, Y. Zheng, Y. Zhu, Q. Liu, Z. Zhang, NLRP3 inflammasome mediated pyroptosis is involved in cadmium exposure-induced neuroinflammation through the IL-1β/IkB-α-NF-κB-NLRP3 feedback loop in swine, Toxicology 453 (2021), 152720.
[61] J. Gao, S. Peng, X. Shan, G. Deng, L. Shen, J. Sun, C. Jiang, X. Yang, Z. Chang, X. Sun, F. Feng, L. Kong, Y. Gu, W. Guo, Q. Xu, Y. Sun, Inhibition of AIM2 inflammasome-mediated pyroptosis by Andrographolide contributes to amelioration of radiation-induced lung inflammation and fibrosis, Cell Death Dis. 10 (12) (2019) 957.
[62] Y. Li, W. Song, Y. Tong, X. Zhang, J. Zhao, X. Gao, J. Yong, H. Wang, Isoliquiritin ameliorates depression by suppressing NLRP3-mediated pyroptosis via miRNA-27a/SYK/NF-κB axis, J. Neuroinflamm. 18 (1) (2021) 1.
[63] M.S.J. Mangan, E.J. Olhava, W.R. Roush, H.M. Seidel, G.D. Glick, E. Latz, Targeting the NLRP3 inflammasome in inflammatory diseases, Nat. Rev. Drug Discov. 17 (9) (2018) 688.
[64] R. Zhou, A.S. Yazdi, P. Menu, J. Tschopp, A role for mitochondria in NLRP3 inflammasome activation, Nature 469 (7329) (2011) 221–225.
[65] H. Jiang, T. Gong, R. Zhou, The strategies of targeting the NLRP3 inflammasome to treat inflammatory diseases, Adv. Immunol. 145 (2020) 55–93.
[66] X. Zhang, A. Xu, J. Lv, Q. Zhang, Y. Ran, C. Wei, J. Wu, Development of small molecule inhibitors targeting NLRP3 inflammasome pathway for inflammatory diseases, Eur. J. Med. Chem. 185 (2020), 111822.
[67] T. Hu, P. Zhu, Y. Liu, H. Zhu, J. Geng, B. Wang, G. Yuan, Y. Peng, B. Xu, PM2.5 induces endothelial dysfunction via activating NLRP3 inflammasome, Environ. Toxicol. 36 (9) (2021) 1886–1893.
[68] M.T. Song, J. Ruan, R.Y. Zhang, J. Deng, Z.Q. Ma, S.P. Ma, Astragaloside IV ameliorates neuroinflammation-induced depressive-like behaviors in mice via the PPARγ/NF-κB/NLRP3 inflammasome axis, Acta Pharmacol. Sin. 39 (10) (2018) 1559–1570.
[69] N. Özenver, T. Efferth, Phytochemical inhibitors of the NLRP3 inflammasome for the treatment of inflammatory diseases, Pharm. Res. 170 (2021), 105710.
[70] K. Schroder, J. Tschopp, The inflammasomes, Cell 140 (6) (2010) 821–832.
[71] T. Strowig, J. Henao-Mejia, E. Elinav, R. Flavell, Inflammasomes in health and disease, Nature 481 (7381) (2012) 278–286.
[72] T. Bergsbaken, S.L. Fink, B.T. Cookson, Pyroptosis: host cell death and inflammation, Nat. Rev. Microbiol 7 (2) (2009) 99–109.
[73] B.E. Burdette, A.N. Esparza, H. Zhu, S. Wang, Gasdermin D in pyroptosis, Acta Pharm. Sin. B 11 (9) (2021) 2768–2782.
[74] M. Lamkanfi, V.M. Dixit, Mechanisms and functions of inflammasomes, Cell 157 (5) (2014) 1013–1022.